Navigation with IMU and Magnetometer

Introduction:

In addressing positioning challenges within changing environments, a variety of devices can be employed, each with their unique benefits and limitations. For this lab, we utilized the VN-100 Inertial Measurement Unit (IMU) to gather data from accelerometers, gyroscopes, and magnetometers, alongside a GPS Receiver for capturing positioning information. Subsequent steps were undertaken to adjust and process this data to determine the projected trajectory of a drive around Northeastern University for each device. Ultimately, this allowed us to deduce the accuracy and effectiveness of both the IMU and GPS devices in determining exact positioning data.

In this lab, we navigated Northeastern University and gathered data using both an IMU and a GPS device. The positioning of these devices was crucial for accurate data acquisition, necessitating specific orientations. We mounted the IMU device on the car's dashboard, ensuring it was fixed at a zero-degree angle with its x-axis directly forward. This orientation was vital because our preliminary assumption was that we were operating in a 2D plane, with the x-direction consistently aligned with the vehicle's trajectory. Following this, we positioned the GPS device directly above and aligned with the IMU, minimizing any obstructions to the GPS's communication with satellites and enhancing the precision of the datasets from both devices.

I developed two device drivers that collected, sifted through, and relayed data from each sensor to a ROS (Robot Operating System) topic. We then recorded these topics onto a ROS bag for further analysis.

Data Analysis:

By examining the data from the ROS topics, we managed to identify and adjust key parameters that described our vehicle's movement. Graphical representations of this data are displayed in the sections below:

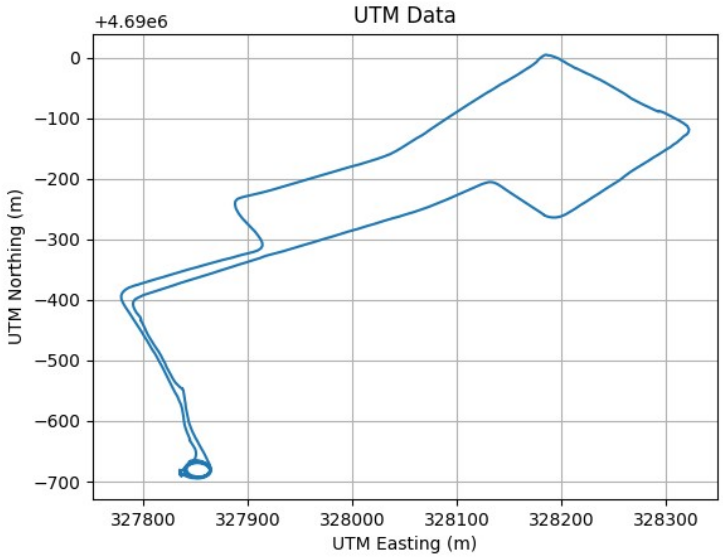

Fig 1: UTM Northing vs UTM Easting

The Figure 1 above shows the plotting of the UTM Data with UTM Northing vs UTM Easting. The values have been plotted from the ROS bag. It indicates the mapping of the data from the ros topics and process the data to determine the projected trajectory of a drive around the Northeastern University for each device.

Heading Correction:

We adjusted the vehicle's heading, or the yaw angle, by considering the hard-iron and soft-iron distortions in the magnetometer data. Figure 2 below shows the data for the X and Y Magnetometer.

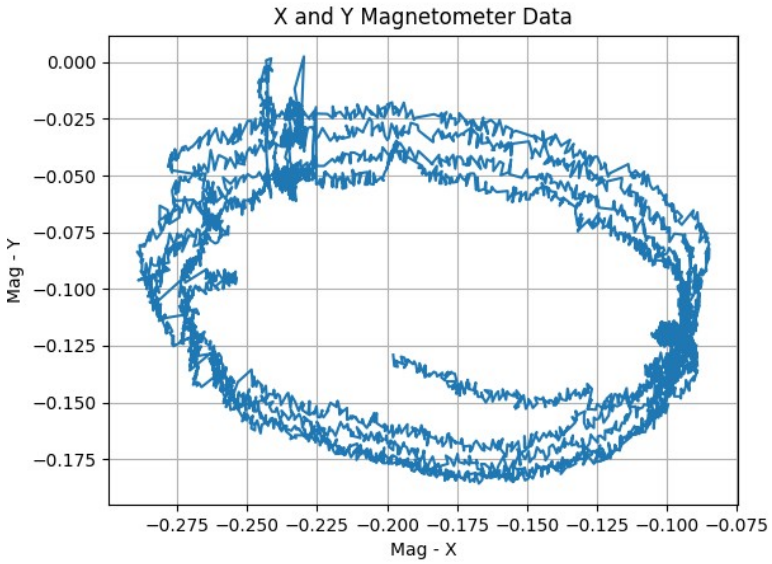

Fig 2: X and Y Magnetometer Data

Hard iron distortions stem from changes in magnetic field data linked to the sensor's location, often manifesting as a persistent deviation from the magnetometer's true zero.

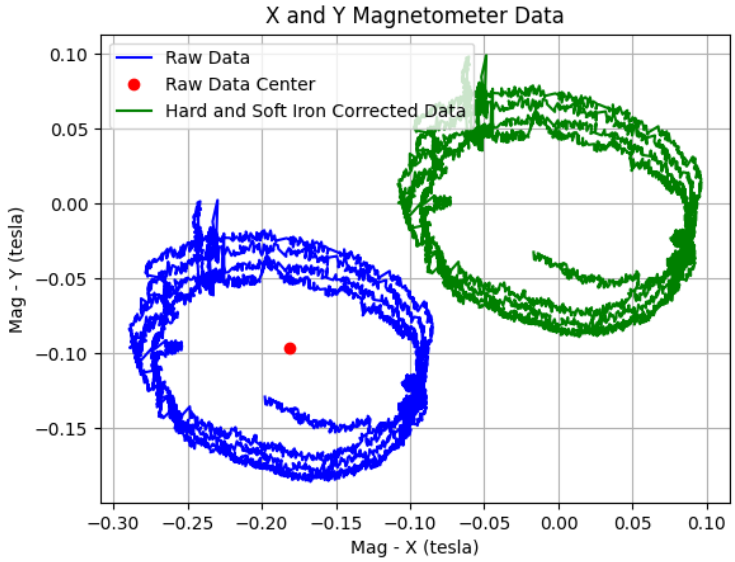

Fig 3: Data Corrected for Hard Iron and Soft Iron Distortions

On the other hand, soft iron effects distort the existing magnetic field, which can be observed as stretching or skewing of the magnetic field. These influences can be visually represented and rectified by graphing the magnetometer data. Figure 3 above displays the initial magnetometer data along with the data corrected for hard iron and soft iron distortions. Utilizing the adjusted magnetometer data, I calculated an estimated yaw angle for each Magnetic Field X and Y pair using the following formula:

$$yaw = arctan2(Mx / My)$$

Additionally, I derived another yaw estimate by integrating the Z-axis angular velocity from the IMU device. The integration of angular velocity results in the angle, and the rotation about the Z-axis determines the yaw angle, considering the IMU device's orientation during data collection. Subsequently, I applied a complementary filter to both yaw estimates using the equation:

$$filter = 0.9 * (integrated\ yaw) + 0.1 * (magnetometer\ yaw)$$

The graph below Figure 4 shows the corrected yaw data for the two yaw calculations i.e for the corrected magnetometer and angular integrated.

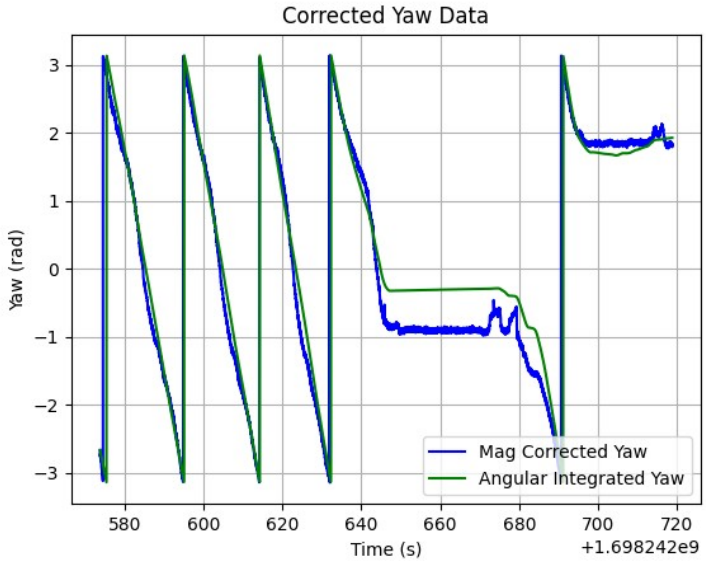

Fig 4: Two Yaw Calcualtions

From Figure 5 below, it's evident that the yaw derived from the corrected magnetometer calculation exhibits more noise compared to the integrated angular rate. This primarily arises from the magnetometer's heightened sensitivity to external factors during data collection that influence its output. In contrast, the integrated angular rate calculation presents a smoother and more precise yaw angle representation. However, it's prone to gradual drifting over time due to the integration process. The primary purpose of computing the complementary filter is to harness the strengths of both the integrated angular rate and corrected magnetometer data calculations to achieve the most accurate final outcome. Consequently, we implement a high-pass filter on the integrated angular rate calculation and a low-pass filter on the magnetometer calculation, then merge the two for a precise yaw angle estimation throughout our data gathering.

Plots of all three yaw calculations are seen below:

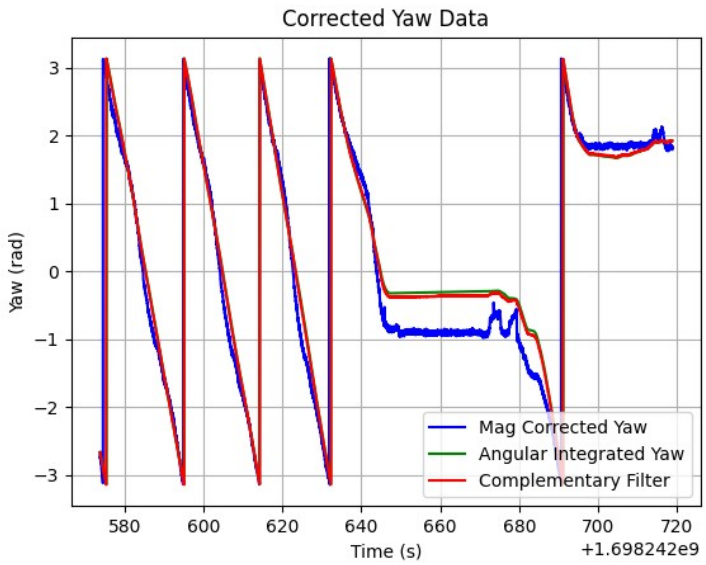

Fig 5: Three Yaw Calcualtions

As depicted in Figure 6 below, our complementary filter yaw calculation aligns almost perfectly with the yaw directly calculated from the IMU, with minor discrepancies attributable to external factors that introduced noise in the magnetometer calculations.

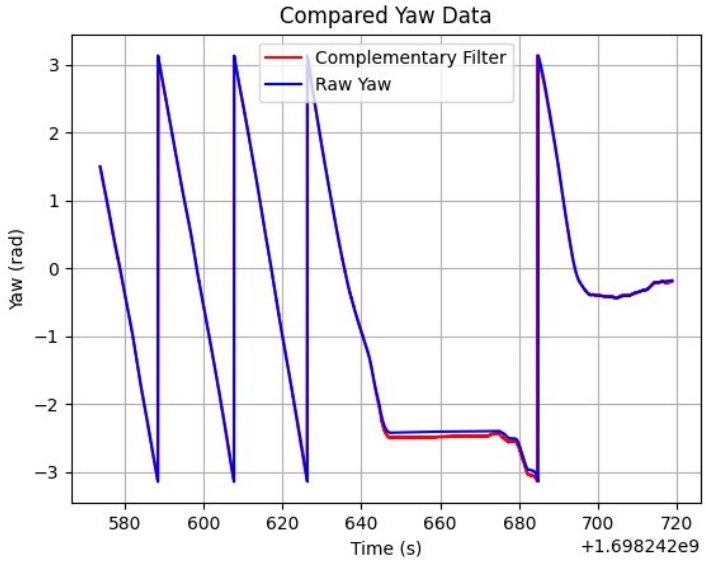

Fig 6: Raw Yaw from IMU and Complementary Filter Yaw

Estimating Velocity:

The IMU acceleration is not perfectly calibrated, the error can be seen in the data since the acceleration data is close to zero. This is due to few factors. Initially, there's an inherent bias in the accelerometer readings. The device experiences gravitational acceleration, and since our IMU wasn't perfectly horizontal during the entire journey, this acceleration contributed to the X-direction acceleration throughout data collection. Furthermore, sensor noise needs to be mitigated. The accelerometer isn't entirely stable when stationary due to its high sensitivity.

To minimize these issues and achieve a more accurate depiction of the IMU acceleration, I started by deducting the average bias from the stationary data collected at the beginning of the route from the X-direction acceleration values. Upon analysis, I noticed a consistent drift in the integrated IMU data that directly paralleled the GPS-derived position data. I established a new baseline for the integrated values, illustrated in red in Figure 7 below, and based the integrated calculations on this new baseline. Additionally, I set values indicating velocities below zero to 0, as there was no reverse movement. The results post-adjustment, alongside the original IMU and GPS velocity calculations, are displayed in Figure 7.

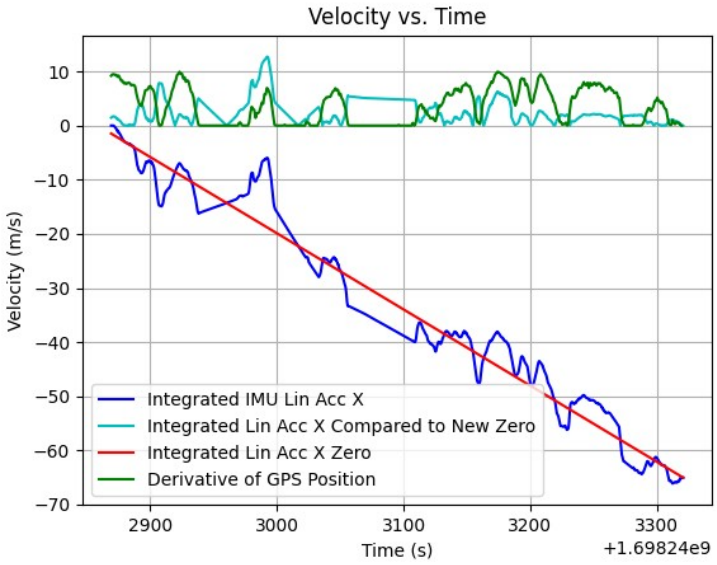

Fig 7: Adjusted IMU Velocity Estimate

Estimating Vehicle Trajectory:

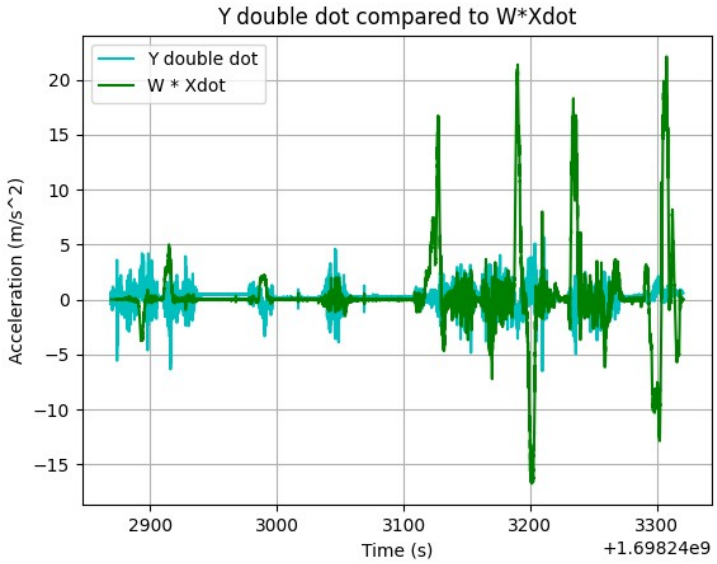

Fig 8: Comparison between Y lin acc, Yaw rate Z and X velocity after adjustments

Having attained precise estimates of the vehicle's orientation and velocity during our drive, we can now deduce its trajectory. Our initial step involves comparing theoretically accurate values to identify potential errors and their causes. We examine the relationship between the linear acceleration in the Y direction (Y double dot), the yaw rate around the Z axis (Wz), and the velocity in the X direction (X dot), as recorded by the IMU. The association among these variables is expressed by the formula:

$$Y\ double\ dot = Wz * X\ dot$$

As evident from Figure 8 above, the graphs exhibit both similarities and differences. In terms of similarities, they share the same overall shape. Peaks in the linear acceleration in the Y direction recorded by the IMU correspond to similar spikes in the angular rate Z and X velocity graph, illustrating the connection between these parameters and Equation. The notable differences stem from factors previously mentioned. There's an apparent bias offset in the IMU's observed Y acceleration, primarily due to the gravitational linear acceleration component in the Y direction during the drive. Another disparity arises because the integrated acceleration in the X direction, or Xdot, has been cleansed of the gravitational bias and modified to align more closely with the GPS data. Since the Xdot values used in this calculation have been adjusted to remove the bias and diminish noise, the measurements exhibit less error than those directly observed by the IMU device. This leads to reduced noise in the graph in Figure 8.

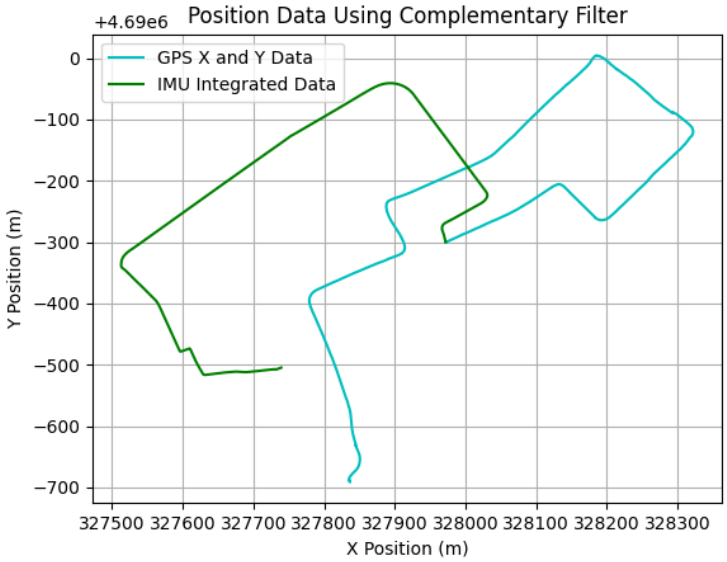

Fig 9: Estimated Trajectory using a Complementary Filter, Flipped and Rotated 105 Degrees

As demonstrated above, the estimated trajectory using a complementary filter, depicted in Figure 9, more accurately reflects the vehicle's true trajectory. This is attributed to the factors discussed earlier in the section accompanying Figure 5. Figure 9 highlights several key strengths and weaknesses of utilizing IMU devices in navigation.

One noticeable observation is that at several turning points in the route, the trajectory estimated by the IMU device tends to exceed that of the GPS route. This discrepancy primarily stems from the differences highlighted in Figure 7. Initially, the trajectory closely aligns with the GPS route, but as disparities accumulate between our projected velocity calculations, the deviation between the IMU and GPS estimated trajectories begins to widen. Nonetheless, the overall shapes of both trajectories are

strikingly similar. This indicates that the yaw calculations performed by the complementary filter are highly accurate.
The computations presented in Figure 8 above operate under the presumption that the vehicle's center of mass aligns with the vehicle frame. In scenarios where this assumption does not hold, Eq. 3 is extended to...

$$\acute{x}_{obs} = \acute{X} - \omega \acute{Y} - \omega^2 x_c$$
$$\acute{y}_{obs} = \acute{Y} + \omega \acute{X} + \acute{\omega} x_c$$

Under the assumption that there was no horizontal sliding in the Y direction, leading to accelerations and velocities in that direction being considered zero, Eq. 7 can be manipulated and resolved to estimate the position of the IMU device in relation to the vehicle frame, resulting in:

$$x_c = 0.833 \text{ m}$$

Conclusion:

Both IMU and GPS devices are exceptionally valuable technologies for positioning, yet each has its own strengths and limitations in various scenarios. This study clearly demonstrates that GPS devices unsurprisingly excel in positioning accuracy over extended distances and timeframes compared to data from IMU devices. However, IMU devices have shown remarkable efficiency in precisely detecting minor changes in vehicle orientation, even over prolonged periods. Recognizing these advantages, along with understanding the impact of noise, gravity, and other external influences on raw data, is vital for effectively utilizing these devices for positioning purposes. When employed together appropriately, they offer the essential technology for accurately determining the positioning and orientation in numerous robotic applications.